

Using Reservoir Computing to Predict a Macroscopic Signal

A. V. Andreev^{a, b, *}, V. M. Antipov^{a, b}, and A. A. Badarin^{a, b}

^a Neuroscience and Cognitive Technology Laboratory, Innopolis University, Innopolis, 420500, Russia

^b Baltic Center for Neurotechnology and Artificial Intelligence, Immanuel Kant Baltic Federal University, Kaliningrad, 236041 Russia

*e-mail: andreevandre1993@gmail.com

Received April 20, 2023; revised May 22, 2023; accepted June 28, 2023

Abstract—The authors study the ability of reservoir computing to predict a complex macroscopic signal with chaotic dynamics. To improve the efficiency of prediction, the phase space of the signal is reconstructed by adding delays. Characteristics of predictions and the parametric space of reservoir are studied, depending on the number of delays.

DOI: 10.3103/S1062873823703616

INTRODUCTION

The application of radiophysics, nonlinear dynamics, and artificial intelligence to problems of neurophysiology is an important trend in modern science [1–5].

Complex systems are characterized by multiple interacting spatial and temporal scales that challenge classical numerical means in predicting and controlling their dynamics. In real life, we are faced with problems of predicting dynamics of different nature, e.g., weather, climate [6], medicine [7], and neuroscience [8]. Recurrent neural networks (RNNs) offer a potential way of solving these problems. The most promising RNN for solving such a problem is reservoir computing.

Reservoir computing has been successfully used to predict the chaotic dynamics of Lorentz, Ressler, and Kuramoto–Sivashinsky systems [9–11]. The authors of [11] showed that a neural network with reservoir computing is also capable of modeling the dynamics of such systems. With reservoir computing, the network is trained to reproduce the functional dependence of the system, but since chaoticity is characterized by the divergence of trajectories that differ even slightly under initial conditions, the real and predicted trajectories diverge over time, but the phase patterns of both trajectories remain similar.

We investigated the possibility of predicting a macroscopic signal with chaotic dynamics using such a recurrent neural network as a reservoir. A signal averaged over a network of 100 Kuramoto phase oscillators with adaptive coupling was taken as the initial signal. To improve the efficiency of predicting the dynamics of such a signal, we restored the phase space of the signal by adding phase delays and investigated the effect

the number of delays had on the reservoir efficiency. It was found an excessive growing number of delays intended to restore the original signal did not appreciably alter the prediction of the signal.

MODEL

A model system is a network of 100 Kuramoto phase oscillators, each of which is described by the equation [12]

$$\dot{\phi}_i(t) = \omega_i + \sum_{j \neq i} w_{ij}(t)(\phi_j - \phi_i), \quad (1)$$

where $i = 1, \dots, N$, $\{\omega_i\}$ is a set of random natural frequencies with uniform distribution in the range $[-\pi, \pi]$, and w_{ij} is the strength of the coupling between the i th and j th elements. The sum of the couplings of each oscillator with all other oscillators is 1.

The strength of coupling w_{ij} changes over time according to the adaptive law

$$\dot{w}_{ij}(t) = p_{ij}(t) - \left(\sum_{k \neq i} p_{ik}(t) \right) w_{ij}, \quad (2)$$

$$p_{ij}(t) = \frac{1}{T_m} \left| \int_{t-T_m}^t e^{i(\phi_i(t') - \phi_j(t'))} dt' \right|, \quad (3)$$

where $p_{ij}(t)$ is the average phase correlation between i -th and j th oscillators from time $t - T_m$ to t , with $T_m = 100$ being the characteristic period of memory. Equation (2) describes the process of homophily, while the condition of a constant coupling sum for each oscillator is a property of homeostasis. This model thus describes the dynamics of an adaptive net-

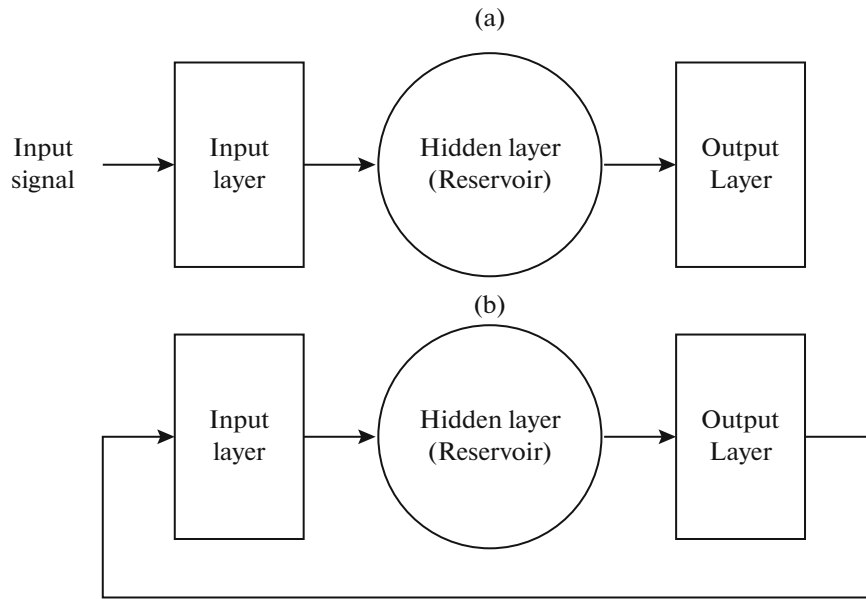


Fig. 1. (a) Model of a recurrent neural network using reservoir computing. In training, an input signal is fed to the input layer of the network, and the connections between the reservoir and the output layer are modified to produce the desired signal at the output layer. (b) In testing, the output of the network is fed to its input layer.

work of oscillators with competition between homeostasis and homophily.

The structure of the recurrent neural network using reservoir computing is shown in Fig. 1. The network has an input layer, a hidden layer (reservoir) and an output layer. The number of neurons in the input and output layers is equal to the number of input signals. Each neuron in the hidden layer is described by the equation

$$\mathbf{h}_t = \tanh(\mathbf{W}_{i,h}\mathbf{I}_t + \mathbf{W}_{h,h}\mathbf{h}_{t-1}), \quad (4)$$

where \mathbf{h}_t is the vector of neuronal states in the reservoir at time t ; $\mathbf{W}_{i,h}$ is the matrix of connections between the input and hidden layers, with the strengths of connections being randomly distributed in the range $[-\delta_{in}, \delta_{in}]$; $\mathbf{W}_{h,h}$ is a matrix of connections between neurons of the hidden layer that forms randomly with specified values of average node degree D and spectral radius R ; and \mathbf{I}_t is the vector of input neuron states at time t (the state of an input neuron is equal to the external signal applied to it). The neurons of the output layer are described by the equation

$$\mathbf{o}_{t+1} = \mathbf{W}_{h,o}\mathbf{h}_t, \quad (5)$$

where \mathbf{o}_t is the vector of neuronal states in the output layer at time t , and $\mathbf{W}_{h,o}$ is the matrix of connections between the hidden and output layers.

The number of neurons in the reservoir is set at 1000. At the beginning, all connections between the reservoir and the output layer are 0. The connections between the input layer and the reservoir are uniformly distributed so that each neuron in the reservoir is connected to only one input neuron, and the number of

connections of all input neurons is approximately equal. There are no connections within the input and output layers.

During the learning process (Fig. 1a), input signals are successively fed to the input layer. Each of signal changes the output links to produce the target value. In predictions, the output value corresponds to the exact value of the input signal following the one presented at a given iteration; i.e., the output signal is the input signal shifted 1 step forward.

In the learning process (Fig. 1b), the initial value of the signal is fed to the input of the network. The output value of the neural network is then fed to the input, starting from the first iteration. The network thus becomes closed, allowing it to autonomously generate a signal based on its knowledge of the initial signal and functional dependence obtained while learning.

RESULTS AND DISCUSSION

We investigated the possibility of predicting the macroscopic dynamics of a network of $N_o = 100$ Kuramoto phase oscillators with adaptive links using reservoir computing. The chosen size of the network is due to the ability of this number of oscillators to obtain a complex chaotic macroscopic signal. The signal averaged over the entire Kuramoto oscillator network is used as the macroscopic signal. The initial macroscopic signal had duration $T = 10000$ s with time step $\Delta t = 0.1$ s. It was calculated as

$$X_{avr} = \frac{1}{N_o} \sum_{i=1}^{N_o} \sin[\phi_i(t)]. \quad (6)$$

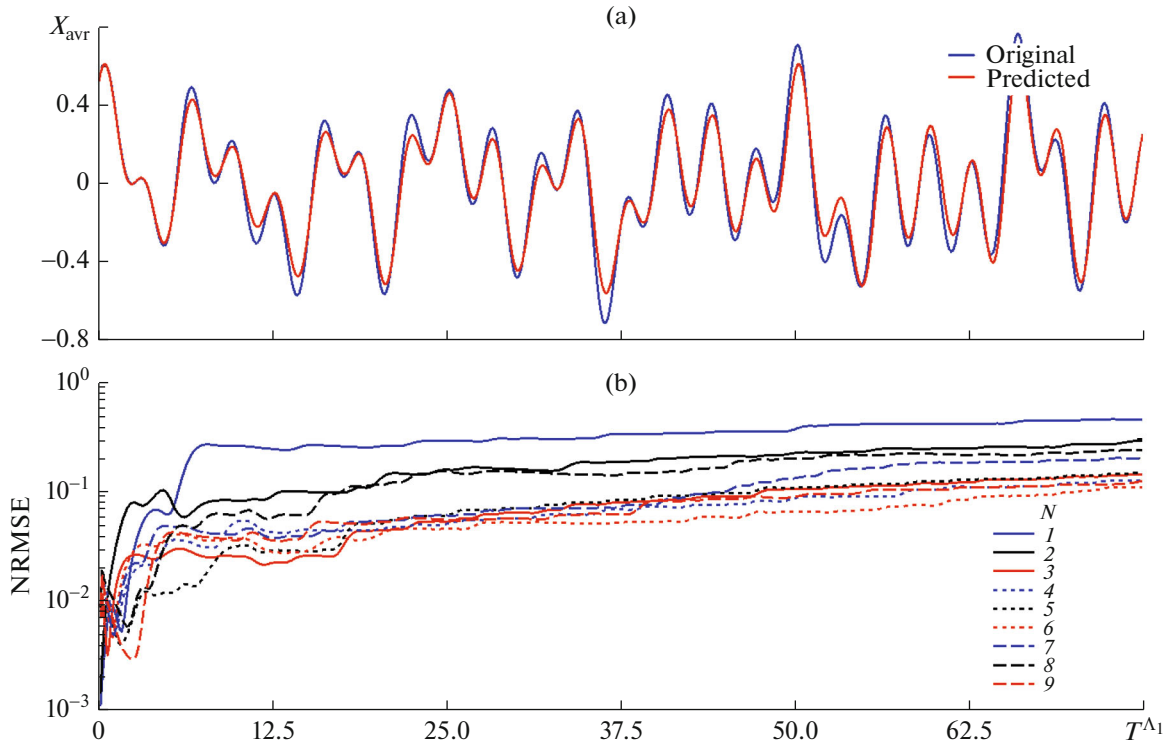


Fig. 2. Timeline of original and predicted signals: (a) when 3 signals (original + 2 delays) are input to the network; (b) with normalized root-mean-square errors NRMSE for different numbers of input signals N .

This signal was divided into two equal parts of 5000 s duration each: the first part of the signal was used during network training, while the second part was used during testing.

To study the characteristics of the macroscopic signal, the highest Lyapunov exponent on the time realization is calculated according to the procedure described in [13]. Point x_0 is chosen on the resulting initial time. Point x'_0 is found close by at $\|x'_0 - x_0\| = \varepsilon_0$, but not close in time to point x_0 . Two time series are considered until distance ε'_0 between two points in these series (x_1 and x'_1) exceeds some ε_{max} . At this point, time T_1 between points x_1 and x_0 and ratio $\varepsilon'_0/\varepsilon_0$ are recorded, point x''_1 is chosen close to x_1 at distance $\|x''_1 - x_1\| = \varepsilon_1$, and the algorithm is repeated. As a result, the highest Lyapunov exponent is calculated as $\Lambda_1 = \left(\sum_{k=0}^{K-1} \ln(\varepsilon'_k/\varepsilon_k) \right) / \left(\sum_{k=0}^{K-1} T_k \right)$, where K is the number of algorithm repetitions.

The calculated highest Lyapunov exponent was $\Lambda_1 = 0.8$, which testifies to the chaotic dynamics of the considered signal (because $\Lambda_1 > 0$). For convenience in analyzing the dynamics of the signal, we used Lyapunov time, calculated as $T^{\Lambda_1} = 1/\Lambda_1 = 1.25$.

It was found that the use of such a signal without applying additional means does not allow to train the reservoir to predict its dynamics. To improve the efficiency of predicting the dynamics, the dimensionality of the phase space of the original signal was estimated according to the false nearest neighbor [14]. It was restored using a time delay by adding additional signals shifted relative to the original one by 4.5 s [13] to increase the number of original signals related to each other.

It was calculated that the dimensionality of the phase space for the considered macroscopic signal was 2.8, so the phase space was restored to dimensionality 3. It should be noted that raising the number of oscillators will increase the complexity of the macroscopic signal dynamics and probably the dimensionality of the phase space as well. This would require more delays for effective prediction. On the other hand, calculating the macroscopic signal over a smaller number of oscillators is impractical. Figure 2a shows a prediction obtained using the reconstructed phase space. As can be seen, this approach allows the signal to be predicted quite accurately within 50 Lyapunov times. The reservoir reproduces all phases of the signal quite well, with only one small error in the accuracy of reproducing the amplitude of oscillation.

The effect the number of delays had on the reservoir's performance was investigated next. The normal-

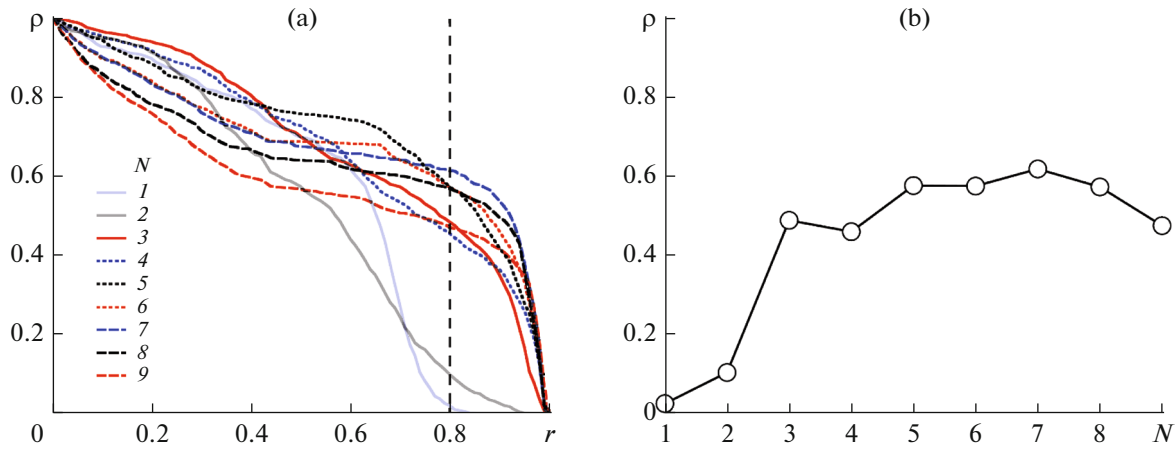


Fig. 3. (a) Dependence of the fraction of points in parameter space (D, R, δ_{in}) , with correlation between the original and predicted signals greater than r , on r for different numbers of input signals N ; (b) values of these fractions when $r = 0.8$.

ized RMS error between the original and predicted signals was calculated as

$$\text{NRMSE} = \sqrt{\frac{\frac{1}{n} \sum_{i=1}^n (o_i - \hat{o}_i)^2}{\sigma_o^2}}, \quad (7)$$

where o is the original signal, \hat{o} is the predicted signal, and σ_o is the standard deviation.

Figure 2b shows the dependences of normalized root-mean-square errors (NRMSEs) on Lapunov time for different numbers of input signals. We can see the NRMSEs first grow rapidly, reach the stationary level set for each number of input signals, and then grow slowly over time. It is noteworthy that the NRMSEs for one and two input signals are considerably greater than the other number of signals converging to similar values over time.

We may conclude that adding two delays to the reservoir input greatly improves the quality of predicting, while adding more signals barely alters it. To investigate what happens when the number of delays is raised from 2 to 8, we analyzed the parameter space (average node degree D , spectral radius R , input correlation scaling factor δ_{in}) and calculated the fraction of points with correlation exceeding certain value r :

$$\rho = \frac{N_r}{N_{all}}, \quad (8)$$

where N_r is the number of points with correlation exceeding r ; r is the Pearson correlation between the original and predicted signals time interval from 0 to $75 T^\wedge$; and N_{all} is the total number of points in the parameter space.

Figure 3a shows dependences ρ obtained for different numbers of input signals. It is obvious that the dependences for $N = 1$ and 2 behave differently from the others: they first change weakly as r falls. They

begin to grow rapidly when $r = 0.8$, and the rapid growth is replaced by a slow increase at $r = 0.5$. The dependences obtained for any other number of input signals (3 or more) display different behavior: they immediately begin to grow rapidly as the correlation falls, but rapid growth is followed by a slow increase at $r = 0.9$.

It is also noteworthy that the number of points in the parameter space with high correlation r falls as the number of input signals rises. This is illustrated in Fig. 3b, which shows dependence ρ of on the number of input signals when $r = 0.8$. The low ρ values for $N = 1$ and 2 are due to the low correlation that can occur with such N values, and to the poor performance in predicting.

It is clear that raising the number of input signals from 3 to 9 has virtually no effect on the number of optimal points in the parameter space with high correlation (Fig. 3b). We may assume this was due to the dimensionality of the phase space of the original signal. Adding two delays to the reservoir input fully restored the phase space. The structure of the signals was complete and predictable for the reservoir. Raising the number of signals thus does not add any unknown information that can be useful for predicting.

CONCLUSIONS

We investigated the possibility of using such a recurrent neural network for reservoir computing to predict a macroscopic signal with chaotic dynamics. The latter was modeled with a signal averaged over 100 Kuramoto phase oscillators coupled by adaptive links.

It was shown that effective prediction requires the phase space of the original signal to be reconstructed by adding delays to it. We investigated the effect the number of delays has on the reservoir efficiency. It was found that raising the number of delays more than is

needed to reconstruct the original signal does appreciably alter either the accuracy of prediction or the number of optimal reservoir parameters at which a good correlation between the original and predicted signals can be obtained.

FUNDING

This work was supported by RF Presidential Grants no. MK-580.2022.1.6 and NSh-589.2022.1.2.

CONFLICT OF INTEREST

The authors declare that they have no conflicts of interest.

REFERENCES

1. Betzel, R.F., Gu, S., Medaglia, J.D., et al., *Sci. Rep.*, 2016, vol. 6, p. 30770.
2. Hramov, A.E., Koronovskii, A.A., Makarov, V.A., et al., *Wavelets in Neuroscience*, Heidelberg: Springer, 2015.
3. Kuc, A., Korchagin, S., Maksimenko, V.A., et al., *Front. Syst. Neurosci.*, 2021, vol. 15, p. 1.
4. Frolov, N. and Hramov, A.E., *Chaos*, 2021, vol. 31, no. 10, p. 101106.
5. Makarov, V.V., Zhuravlev, M.O., Runnova, A.E., et al., *Phys. Rev. E*, vol. 98, no. 6, p. 062413.
6. Weyn, J.A., Durran, D.R., and Caruana, R., *J. Adv. Model. Earth Syst.*, 2019, vol. 11, no. 8, p. 2680.
7. Esteva, A., Kuprel, B., Novoa, R.A., et al., *Nature*, 2017, vol. 542, no. 7639, p. 115.
8. Bzdok, D. and Ioannidis, J.P., *Trends Neurosci.*, 2019, vol. 42, no. 4, p. 251.
9. Vlachas, P.R., Byeon, W., Wan, Z.Y., et al., *Proc. R. Soc. A*, 2018, vol. 474, no. 2213, p. 20170844.
10. Pathak, J., Wikner, A., Fussell, R., et al., *Chaos*, 2014, vol. 28, no. 4, p. 041101.
11. Griffith, A., Pomerance, A., and Gauthier, D.J., *Chaos*, 2019, vol. 29, no. 12, p. 123108.
12. Makarov, V., Koronovskii, A.A., Maksimenko, V.A., et al., *Chaos, Solitons Fractals*, 2016, vol. 84, p. 23.
13. Kuznetsov, S.P., *Dinamicheskii khaos* (Dynamic Chaos), Moscow: Fizmatlit, 2001.
14. Rhodes, C. and Morari, M., *Phys. Rev. E*, 1997, vol. 55, no. 5, p. 6162.

Translated by M. Hannibal